

DYNAMIC TESTING OF AUTOCLAVED AERATED CONCRETE BLOCK MASONRY BUILDING MODELS

Sharadkumar P. Purohit (Corresponding Author)
Professor, Civil Engineering Department, School of Engineering
Institute of Technology, Nirma University, Ahmedabad, Gujarat, India
E-mail: sharad.purohit@nirmauni.ac.in

Sharad. V. Senjaliya
Former Postgraduate Student, Civil Engineering Department, School of Engineering
Institute of Technology, Nirma University, Ahmedabad, Gujarat, India
E-mail: 16mclc20@nirmauni.ac.in

ABSTRACT

Masonry buildings made from passive stone/brick materials are acceleration sensitive and vulnerable to seismic forces. Current construction practices see a surge in use of light weight Autoclaved Aerated Concrete (AAC) blocks. This paper studies dynamic behavior of semi-engineered AAC block masonry building models under shock loading. Two half-scale models are constructed practicing half-block joint (English bond) and full-block joint (Stretcher bond) on a unique semi-automated shock table facility. Dynamic response of long and short walls of building models are measured with reference to base excitation. Building model built with stretcher bond survives despite suffered with heavy damage and perform better than model with English bond which collapsed under series of shock loading. Long walls of models observe major damage due to out-of-plane bending modes, shear cracks and vertical separation at wall junction. Peak acceleration response of long walls shows reduction with progression of damages with reference to base excitation. Performance of AAC block masonry building is found to be at par with red-clay brick masonry building studied previously.

KEYWORDS: Semi-Engineered Masonry Building; Autoclaved Aerated Concrete Block; Shock Table; Dynamic Testing

INTRODUCTION

Non-engineered masonry building is a common typology used world-wide for human habitat. Past earthquakes have proved that masonry buildings perform poorly and have attracted heavy damage causing human and capital losses. One of the reasons for damage to masonry building is its massiveness which attracts large acceleration and thus large lateral force. Current construction practices employ Autoclaved Aerated Concrete (AAC) blocks instead of red-clay bricks as masonry infill in Reinforced Concrete (RC) buildings due to its low weight and greater flexibility to the construction. AAC block is a light weight concrete with pores and is also known as Autoclaved Cellular Concrete (ACC), Autoclaved Lightweight Concrete (ALC), Porous Concrete and Thermalize Concrete. The commercial AAC blocks are of two types: sand based and fly-ash based with compressive strength ranges between 3 to 4.5 MPa when tested following IS:2185 (Part -3) - 1984 [1]. AAC block is almost 2.25 times lighter as compared to red-clay brick and 2 times lighter than fly-ash brick. Its main ingredients include sand, water, quicklime, cement, gypsum, and often, fly ash. The chemical reaction due to the aluminum powder provides AAC its distinct porous structure, lightness and insulation properties that are completely different compared to other lightweight concrete materials.

Recent past have witnessed wide use of AAC blocks as infill materials with Reinforced Concrete (RC) due to its high stiffness to weight ratio and speed of construction. Various research studies attempted in the current decade were focused on behavior of AAC block infilled RC frame panels under lateral loading. Bose and Rai [2] performed displacement controlled slow-cyclic test on reduced scale (1:2.5) single-storey single-bay RC frame to study hysteretic response. AAC infills result in improved load sharing between infill and frame. Non-linear static and dynamic analysis based on FEMAP695 were also performed. Sucuoğlu and Siddiqui [3] tested two concrete frame, one bare and

other infilled with AAC block, under pseudo-dynamic loading. AAC strut model was developed for AAC block masonry infilled frame based on experimental results. Shear failures in term of diagonal cracking and corner crushing were observed and thus shear is required to be considered for boundary column design.

Schwarz et al. [4] investigated influence of non-structural masonry infill walls on seismic resistance of RC frames. Low-cycle lateral loadings were applied to RC frame infilled with autoclave-cured aerated concrete blocks. It has been found that various types of masonry infills like red-clay bricks, AAC blocks, and Fly ash bricks improves stiffness of the infilled RC frame significantly and hence lateral load resistance capacity. However, masonry infills rigidly connected to RC frame suffered severe damages [5, 6]. In order to reduce unfavorable interaction between masonry infill and frame as suggested in Chinese seismic code Jiang et al. [7] tested full-scale single-bay single-story RC frame infilled panel of aerated concrete block with flexible connections between frame and infilled wall. Flexible connections helped to improve displacement ductility ratio for the RC frame panel specimens but reduces seismic performances as compared to frame panel with rigidly connected infilled wall.

Few research studies on AAC block masonry buildings through shake table and under in-plane cyclic loadings have been attempted in recent past three-four years. Ersubus and Korkmaz [8] conducted experimental programme on 1/10th scale models of one-storey brick masonry buildings with various strengthening strategies. Economic uniaxial shake table taking cognizance from various such facility used world-wide including one used in the study was developed. Several economic testing techniques used by various researchers to evaluate seismic performance of masonry buildings were summarized. Ghezelbash et al. [9] studied half-scale single-story unreinforced masonry building with asymmetric openings on shake table under bidirectional seismic excitations. Damaged building then retrofitted with steel mesh and different types of shotcrete connections to prove its adequacy by creating strong bond. Costa et al. [10] performed cyclic test on full-scale AAC masonry pier to assess its in-plane behavior. A nonlinear macro-element model was developed for masonry pier and was extended to frame-type macro-element modelling for three dimensional building models. Experimental result showed that ultimate drift limit of 0.3-0.35% can be recommended for the design and shear strength values provided in codes are found to be unrealistically low.

Elmanich and Rabinovitch [11] studied dynamic behavior of AAC masonry walls strengthened with FRP under in-plane loading on shake table. Numerical model using specially tailored 2D elements was developed to study localized effects and coupling between in-plane and out of-plane bending of FRP bonded masonry wall. Miccoli [12] reviewed seismic performance studies of load bearing masonry with AAC under in-plane cyclic loading by various researchers. Unreinforced AAC can face low to medium seismic events with regular geometry. Gokmen et al. [13] studied full-scale two-story building constructed with reinforced-AAC-wall-panel under cyclic loading. It has been found that lateral load capacity of such building increases by 1.6 times its weight with global displacement capacity of around 3.5. Nonlinear static and incremental dynamic analysis were performed on numerical model of the building calibrated from component test results with good agreement. Marino et al [14] demonstrated efficacy of equivalent frame (EF) approach for modelling in-plane seismic response of two unreinforced clay brick masonry buildings damaged during 2010/2011 Canterbury earthquake. Effect of diaphragm stiffness on global response of the buildings were studied.

Few studies on un-reinforced brick masonry buildings using shake table and various retrofitting strategies to such buildings were conducted in India, recently. Nayak and Dutta [15] examined failure patterns of free standing wall (12 nos.) and assembly of four walls (18 nos.) made from half size bricks under swept sine motion. These models were strengthened by PP bands, vertical wire mesh, L-shaped horizontal reinforcing bars and vertical reinforcing bars at corners to provide with simple cost effective seismic enhancement techniques. Chourasia et al. [16] tested single-room masonry building with different typology; unreinforced, reinforced, confined masonry under quasi-static in-plane cyclic loading to address its effectiveness in the Indian context. Experimental results in terms of lateral load capacity, stiffness degradation, displacement ductility capacity and energy dissipation capacities were studied. Kadam and Singh [17] studied half-scale burnt clay brick unreinforced masonry building and similar building retrofitted with Ferro-cement 'splints' and 'bandages' on shock table. Equivalent Frame Model (EFM) of tested scaled models were developed for comparison of numerical results with testing results. Lateral load resistance of retrofitting building was found to improve considerably.

Pathak et al. [18] attempted seismic vulnerability of the Guwahati urban centre due to unscientific transformation of building typology from traditional housing. The damage probability values for various non-engineered masonry were adopted and damage ratios were used to estimate economic losses. A simplified prognostic damage scenario with first-order approximations was proposed.

While studies on brick masonry buildings under lateral loading are relatively very less in India as compared to other countries, similar studies exploring use of AAC block for masonry buildings is in its primitive state of research. In fact, dynamic behavior studies on AAC block masonry building are not yet addressed in the country. The major objective of the present paper is to build two half-scale semi-engineered masonry building using AAC blocks and study its behavior under dynamic loading applied through unique shock table testing facility.

MATERIAL PROPERTIES

Evaluation of physical and mechanical properties of constituent materials of AAC block masonry buildings plays important role in its behavior under dynamic loading. There are two chief constituent materials for AAC block masonry building; AAC block and ready to use Mix-Self Curing Mortar (RMM) binding material. These materials are procured from the bulk manufacturer located in the Ahmedabad region. Material properties are evaluated through series of tests on AAC block unit and mortar cube of RMM at the Heavy Structures Laboratory (HSL).

1 Physical Properties of AAC Block Unit

Physical properties of representative AAC block unit, used for building models, are investigated following IS:2185 (Part 3)–1984 [1] and IS:6441 (Part 1)-1972 [19]. Specimens of size 150 mm × 150 mm × 150 mm are prepared and sample weight are taken. These specimens are then placed for oven drying at 105 ± 5 °C until moisture content is removed and constant weight is achieved within 4 hours. Dry weight of specimens are obtained to determine bulk density and moisture content. Table 1 presents physical properties evaluated for AAC block unit indicating useful data set for AAC block from the region.

Table 1: Physical Properties of AAC Block Unit

Dimensions of AAC Block Unit Specimen (mm)	Bulk Density of the AAC Block Unit Specimen (kg/m³)	Moisture Content (%)	Patten on Surface
150 × 150 × 150	766.42 [#]	19.12 [#]	Zigzag
[#] Values are average over three AAC block unit			

2 Mechanical Properties of AAC Block Unit and RMM

Compressive strength of AAC block unit is determined following stipulations of IS:2185 (Part 3) – 1984 and IS:6441 (Part 5) - 1972. Table 2 shows compressive strength of AAC block units tested on digital compression testing machine. Value in bracket shows CoV (Coefficient of Variation) in %.

Table 2: Compressive Strength of AAC Block Units

Sr. No.	Dimensions of AAC Block Unit Specimen (mm)	Ultimate Load (kN)	Cross-sectional Area of AAC Block Unit (mm²)	Compressive Strength (MPa)	Average Compressive Strength (MPa)
1	150 × 150 × 150	83.70	22500	3.72	4.11 (6.74)
2	150 × 150 × 150	97.60	22500	4.33	
3	150 × 150 × 150	96.35	22500	4.28	

It is evident from Table 2 that average compressive strength of AAC block is found to be lower as compared to red-clay brick strength reported as 4 – 11 MPa [20]; 7.838 MPa [15]; 13.37 MPa [16]; 6 – 8 MPa [21]. However, it can be considered to be at par with fly-ash brick strength reported as 4 – 6 MPa [21]. Note that references are considered from India only to be more relevant in terms of comparison. AAC block unit was failed due to through cracks propagated under concentrated compressive loading and was found to be brittle in nature as it breaks suddenly.

Mortar cubes of size of 70.7 mm × 70.7 mm × 70.7 mm are casted for compressive strength evaluation of RMM binding material following IS:2250 - 1991 [22]. Method of trial and error is adopted to arrive at an optimal water/binder (W/B) ratio since dosage was not specified by the manufacturer. Mortar cubes were tested under compressive load with a uniform loading rate of 2 MPa to 6 MPa on maturity age of 7, 14 and 28 days. A parametric study in terms of different curing conditions for RMM mortar cubes is conducted to assess its curing requirements. One set of test samples (3 nos.) is immersed in the water curing tank while other set is kept in the laboratory for ambient curing at room temperature. Table 3 shows compressive strength of RMM cube samples. Value in bracket shows CoV (Coefficient of Variation) in %.

Table 3: Compressive Strength of RMM used for AAC Block Binding

Sr. No.	Water-Binder Ratio (W/B)	Compressive Strength (MPa)						Curing Method
		7 Days		14 Days		28 Days		
1	0.35	2.85	3.18 (8.37)	4.70	5.03 (10.82)	5.70	5.23 (6.23)	Water Curing
		3.20		5.80		5.02		
		3.50		4.60		5.00		
2	0.35	5.00	5.27 (3.91)	6.40	6.10 (4.82)	6.70	6.93 (2.97)	Ambient Temperature Curing
		5.50		6.20		6.90		
		5.30		5.70		7.20		

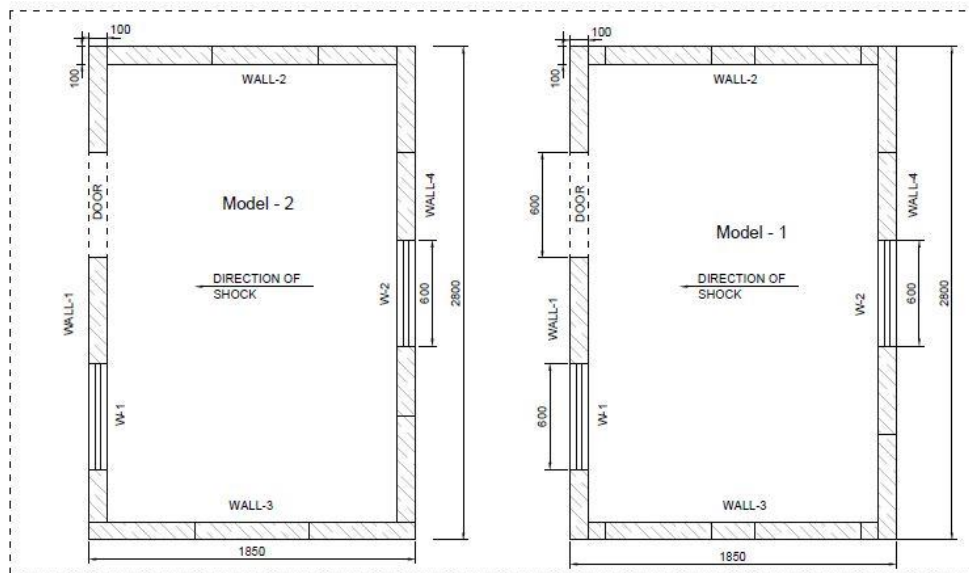
It is evident from Table 3 that ambient temperature curing yields high compressive strength for RMM cubes vis-à-vis normal water based curing. The RMM setting time is as low as 3-4 hours with full strength as compared to normal cement based mortar which takes about 24 hours to achieve its full strength. These are few reasons for faster construction speed achieved when AAC block is used other than its geometrical advantage. RMM is a specialized Ready to Mix – Self Curing cement based Mortar with cement, graded sand and polymeric additives as its constituents to achieve strong mechanical bond as well as adhesion between blocks. Typical proportion practiced is 3 parts of powder with 1 part of water by volume. RMM is a pre-mixed and ready to use which requires only water to be added at the site against lengthy process of site mixing, transport and storage of individual materials for sand cement mortar. It is capable of providing uniform thin bed joint of 3-5 mm (lowest up to 2 mm) with high adhesive strength which improves masonry strength against 10 mm thickness bed joint of conventional mortar. Quantity of mortar used reduces substantially with RMM and raking of joint is not required. Thin layer of RMM joint reduces shrinkage cracks and provides seamless masonry structure. No water curing is required when RMM is used and plastering work can be started after 24 hours of application against 7 days of curing period for conventional sand cement mortar.

RMM cubes show higher compressive strength vis-a-vis AAC block unit which is an expected result due to use of cement and polymer in the mortar. However, in general masonry structures are constructed using the strong unit and weak mortar since strong mortar tends to make the masonry wall too rigid. Strong mortar restricts minor movement of a wall under moisture and temperature variation which causes formation of cracks in the unit. Current study uses polymer based RMM strong mortar being a compatible adhesion solution developed for joining AAC block to improve masonry strength which is conventionally lower.

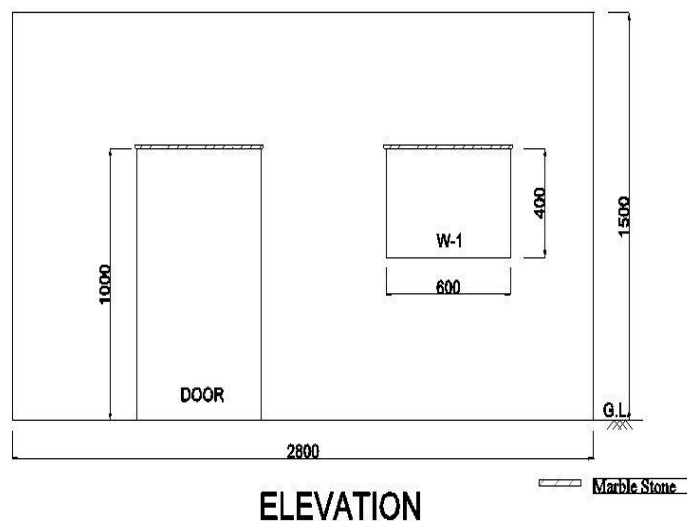
DYNAMIC MODAL TESTING

1 Design and Construction of Scaled Building Models

Two half-scale building models, using AAC blocks, with plan dimensions 2.8 m × 1.85 m are designed with reference to unique shock table facility at the HSL. Unlike non-engineered buildings built with local construction practicing skills, semi-engineered building models are evolved in the form of wall courses and bond between two orthogonal walls with engineering interventions for the present study. Two different types of block bond; half-block joint (English bond) and full-block joint (Stretcher bond) are designed to construct long and short walls, orthogonal to each other, for the building models. Model-1 is prepared with English block bond and Model-2 with stretcher block bond. Long walls of building models are constructed between two sets of L-shaped equal angle steel sections whose one leg connected to concrete slab and other leg standing freely to provide fixity at the base of the wall. Short walls are constructed directly on concrete slab orthogonally connected to long walls. Each long wall of building models is provided with such fixity at the base which worked well during dynamic testing.



(a)



(b)

Fig. 1 Schematic Diagram of Two Half-Scale Masonry Building Models with AAC Block Units (a) Plan with Geometric Dimensions, and (b) Elevation with Dimensions

Figure 1(a) shows schematic diagram of building models plan bearing details of dimensions, wall notations, locations of openings and direction of the shock etc. Figure 1(b) shows elevation of wall W-1 for building models. Building models have been prepared using commercial sand based AAC block of size 600 mm (L) \times 100 mm (D) \times 200 mm (H). Door and two windows of reduced half-scale size are kept in both models to simulate physical attributes of realistic masonry building. Marble stone of 15 mm thickness was provided over door and window openings of building models to form a lintel. To ensure rigid diaphragm action for the building models, modular slab assembly of an equivalent weight against 80 mm thick reinforced concrete slab have been specially fabricated from equal angle steel sections and concrete cubes are placed uniformly in it as shown in Figure 2(d).

Construction of AAC block masonry walls were completed in 3 working days which is almost half of the construction time for red-clay bricks/stones masonry walls constructed for other experimental studies at HSL in the past. Thus, construction of AAC block masonry walls substantially reduces construction efforts. Figure 2 presents various construction phases executed for half-scale building models on unique shock table facility.

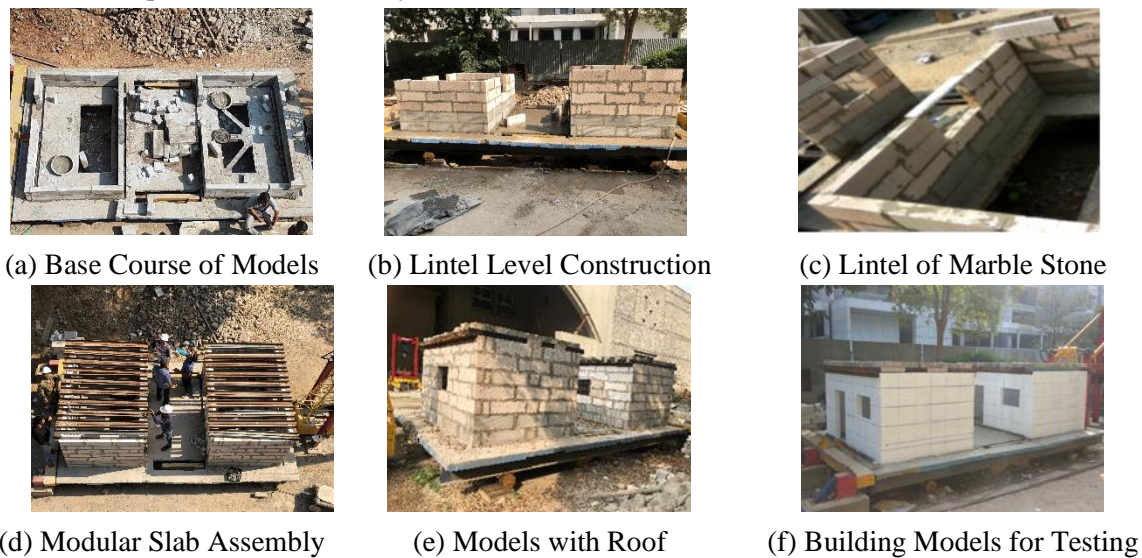


Fig. 2 Construction Phases of Half-scaled Masonry Building Models with AAC Blocks

2 Development of Experimental Set-up

Dynamic response of structures can be well studied by testing scaled model through sophisticated shake table facility in real time. However, high capital and heavy duty maintenance cost makes it non-affordable and thus, various researchers have used semi-sophisticated shock table facility of various forms [8] to study dynamic behavior of structures. In fact, shock table is a much cheaper alternative and still gives good enough insight to the dynamic problem. Shock table facility available at HSL comprises of a freely falling heavy pendulum imparting a shock to the concrete table mounted on roller. Figure 3 shows shock table facility with its components used in the present study as well as in past experimental studies [23]. Unlike in shake table where motion applied is controlled and back and forth, pendulum applies shock to the concrete table only in one direction. However, reaction beam as shown in Figure 3 imparts lower magnitude return shock when concrete table travel past the gap kept between concrete table and reaction beam before application of the shock for high energy impact shocks.

Building models, shown in Figure 2(f), prepared following construction phases as discussed in Section 1, were instrumented with uniaxial accelerometers to measure acceleration at various locations under series of shock loading applied. Long walls of building models constructed perpendicular to the incident shock loading are expected to experience amplified acceleration at its top due to out-of-plane bending vibration. Therefore, 4 nos. of uniaxial accelerometers were attached to each long walls of the building models denoted with notations M1W1, M1W4, M2W1 and M2W4 wherein 'M' stands for model and 'W' for the wall. Short walls, parallel to the shock loading, of large in-plane stiffness are

less likely to suffer acceleration in out-of-plane direction. Thus, 2 nos. of uniaxial accelerometers with notations M1W3 and M2W3 are attached to one short wall of each building model through small steel angle section in the direction of incident shock loading to measure acceleration. One uniaxial accelerometer is attached in the proximity of impact point of freely falling pendulum on the shock table to measure base acceleration imparted to the building models during each shock loading.

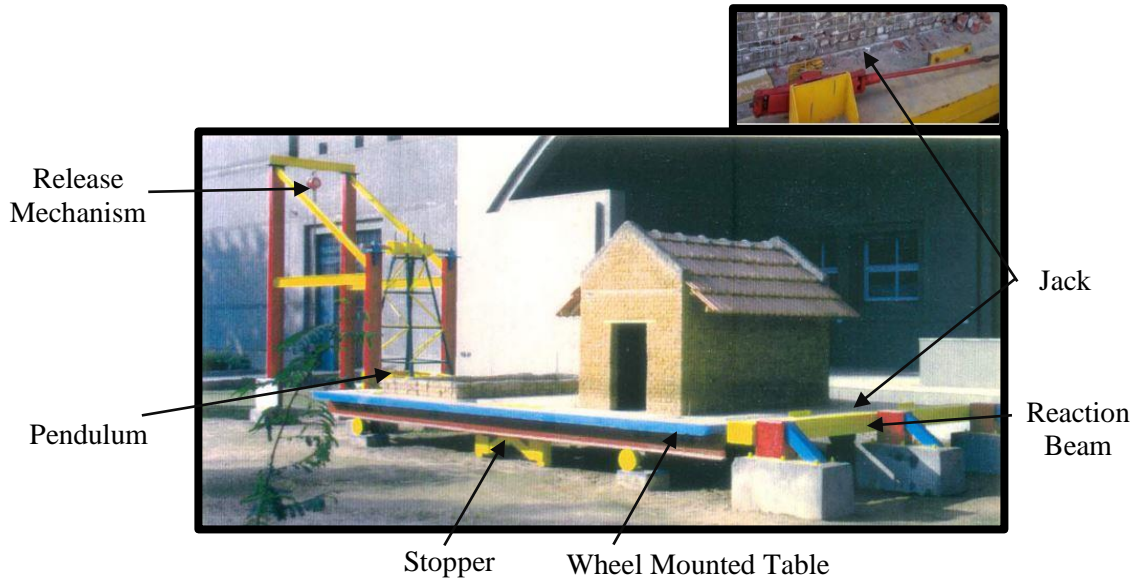


Fig. 3 Semi-sophisticated Shock Table Facility and its Components

Layout of accelerometer network with designated notation and direction of shock loading is shown in Figure 4. Wired uniaxial accelerometers are connected to data acquisition system from National Instruments (NI), USA and computer system to acquire real-time acceleration data during testing of building models and subsequent data processing.

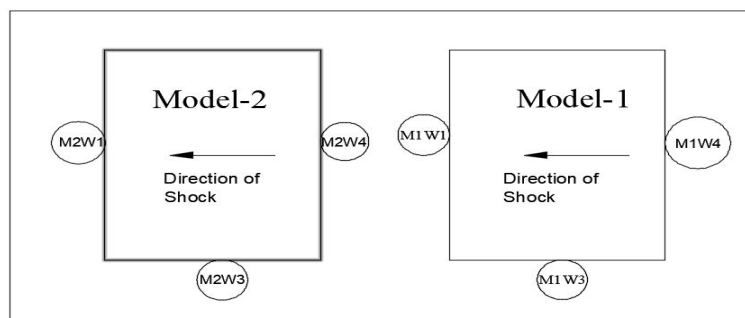


Fig. 4 Instrumentation Layout for Half-Scaled Building Models with Direction of Incident Shock Loading

3 Dynamic Testing of AAC Block based Masonry Building Models

Half-scaled building models constructed on the shock table facility were subjected to series of shock loadings applied through 1.5 Tonne pendulum freely falling with angle of incident ranges from 15° to 45° at an interval of 7.5°. An electrically operated automated pendulum release mechanism was specially developed to ensure smooth release of the pendulum from designated incident angle imparting kinetic energy to the shock table. Real-time acceleration data are acquired through network of accelerometers during each shock loading applied to the building models. Structural damages suffered by each building model were critically observed and were graphically recorded on the blue print of each wall prepared before-hand of the dynamic test. Recorded data were post-processed through LABView software to determine peak acceleration observed by each instrumented wall of building models under base acceleration imparted.

RESULTS AND DISCUSSION

Dynamic behaviour of AAC block based masonry building models tested through shock table facility is measured, both, quantitatively and qualitatively. Recorded acceleration-time history data were analysed to evaluate peak acceleration suffered by the building models. Damages suffered by building models were studied through visual observation after each shock loading, qualitatively. Table 4 reports peak acceleration measured, in terms of ' g ', at top of various walls of building models as well as at base of the shock table under different shocks imparted through the pendulum.

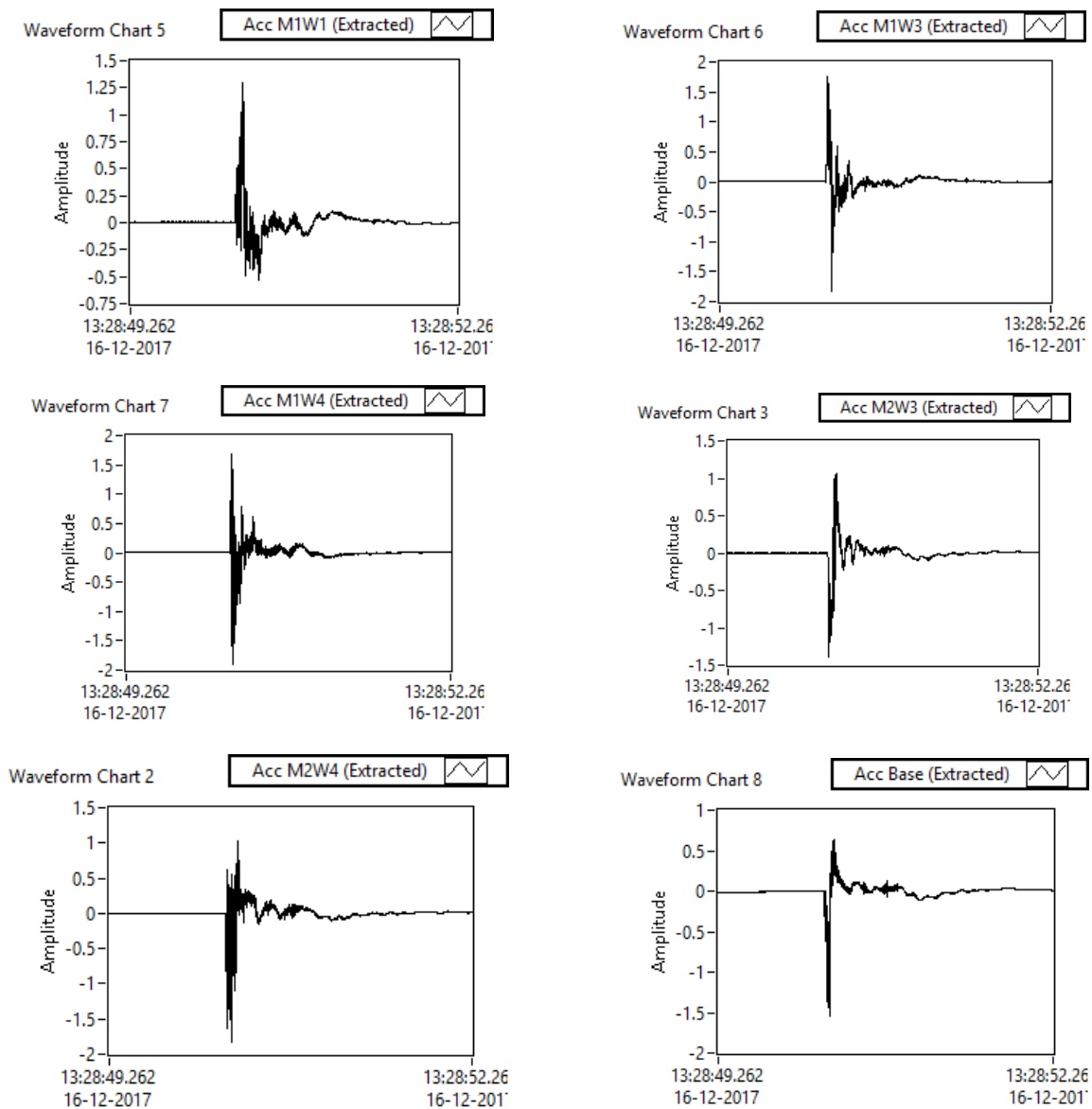


Fig. 5 Time-history Plot of Wall-1, Wall-3, and Wall-4 of Building Models for Shock No. 4 with Impact Angle 22.5°

Impact angle 15° produced same order of peak acceleration at base of building models $0.762g$ and $0.796g$, respectively. Wall-3 of both models showed peak acceleration of the same order that of base acceleration due to its rigidity. However, almost all long walls; wall-1 and wall-4 of building models yield amplification in peak acceleration due to out-of-plane bending and elastic stiffness. Impact Angle 22.5° , with an increment of 7.5° , resulted to $1.007g$ base acceleration with amplification in acceleration in almost all long walls of building models due to presence of minor cracks only. However, repeat

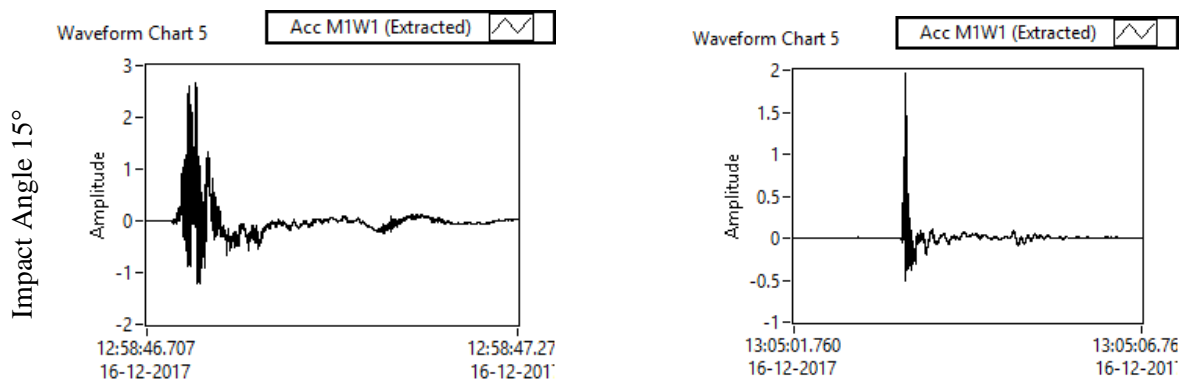
impact angle of 22.5° showed de-amplification in peak acceleration in long wall; wall-1 of building modes due to reduction in elastic stiffness due to presence of cracks of considerable order. Note that, base acceleration increases with increase in impact angle due to increase in impact velocity. Impact angle 30° and 37.5° infused high energy to the building models leading them to heavy damages and thus long walls of building models mostly showed de-amplification in peak acceleration. Short wall; wall-3 of Model-1 suffered with no or relatively low damage and thus peak acceleration showed amplification due to its intact rigidity. De-amplification in peak acceleration of short wall; wall-3 of Model-2 attributed to damage incurred under shock loading. Peak acceleration for impact angle 45° were not measured as accelerometers removed due to heavy damage incurred to building models.

Table 4: Peak Acceleration at Top of the various Walls of the Building Models and at the Base of the Shock Table during Dynamic Testing

Shock No. (Impact Angle)	Peak Acceleration measured at the Top of the Wall, (in 'g')						Peak Acceleration at the Base of the Shock Table, (in 'g')
	Model-1			Model-2			
	Wall-1 (M1W1)	Wall-3 (M1W3)	Wall-4 (M1W4)	Wall-1 (M2W1)	Wall-3 (M2W3)	Wall-4 (M2W4)	
1 (15°)	1.189	0.831	0.499	2.331	0.738	1.344	0.762
2 (15°)	1.927	0.900	0.465	2.645	0.545	1.451	0.796
3 (22.5°)	1.713	1.350	0.394	2.899	0.736	1.409	1.007
4 (22.5°)	1.261	1.762	1.924	1.101	1.389	1.769	1.508
5 (30°)	1.748	2.715	0.794	1.318	1.589	1.390	1.944
6 (30°)	1.392	2.879	2.040	1.093	1.520	0.756	2.500
7 (37.5°)	3.853	2.707	0.594	1.721	2.380	1.457	2.099
8 (37.5°)	2.388	2.152	1.284	2.755	1.429	1.188	2.862

Acceleration data recorded in read-time are plotted for short and long walls of building instrumented with accelerometers under each shock loading applied. Figure 5 shows time-history plot of wall-1; wall-3 and wall-4 of building models and base acceleration under shock no. 4 with impact angle of 22.5°. It is evident that short and long walls of building models showed amplification in peak acceleration at top of the wall to base acceleration.

To understand dynamic behaviour of building models, time-history plot of each short and long wall were plotted for each shock loading. Figure 6 shows time-history plot of long wall; wall-1 of Model-1 at different stages (impact angle 15°-37.5°) of shock loading. Time-history plots for other short and long walls of building models were plotted but difficult to accommodate here.



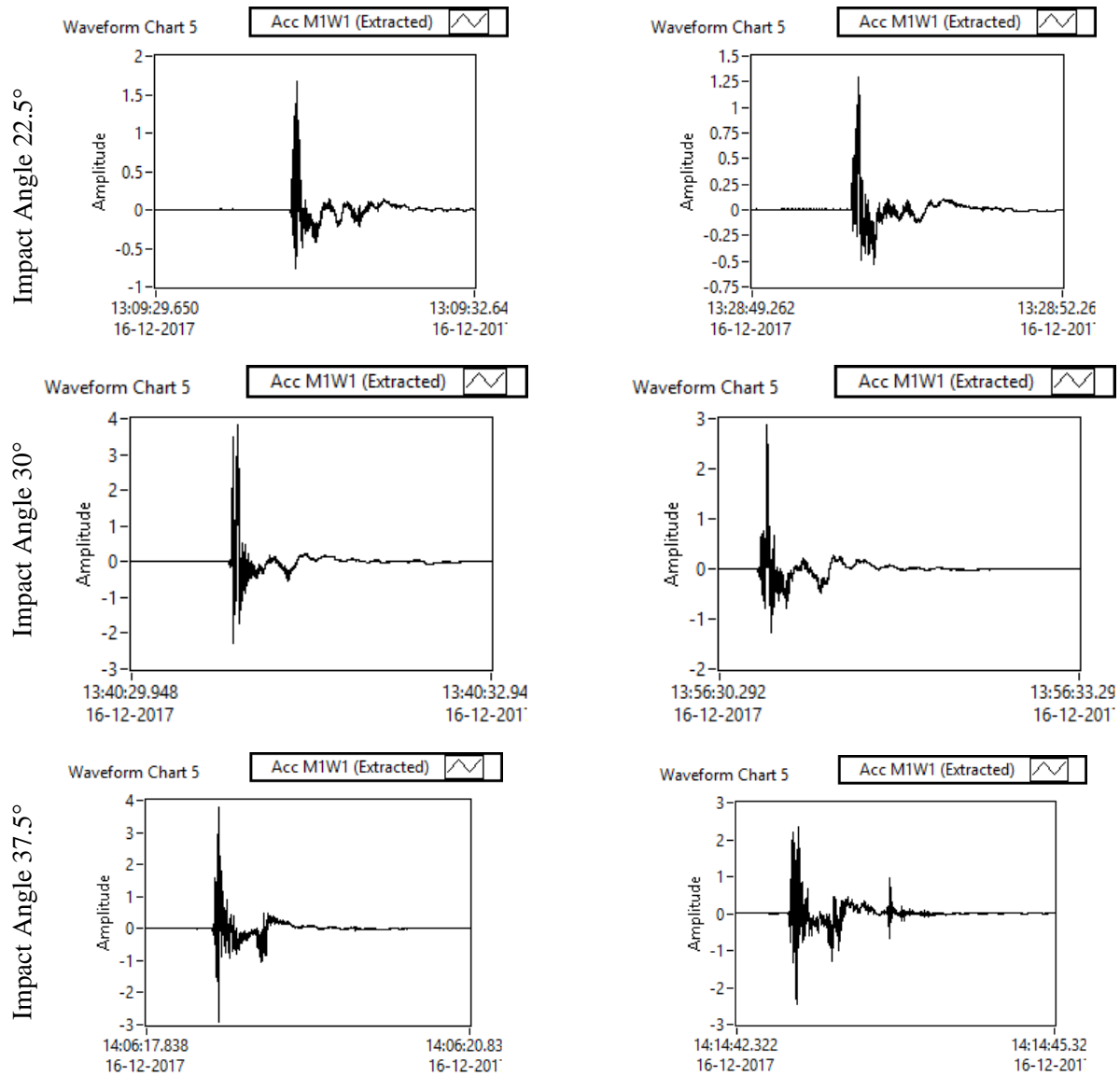


Fig. 6 Time-history Plot of Wall-1 of Model-I at Different Stages of Shock Loading

Building models have been critically observed after each shock loading applied to assess damage suffered by AAC block masonry short and long walls. Table 5 tabulates critical observation on damage patterns of building models under each shock loading with possible reasons for it.

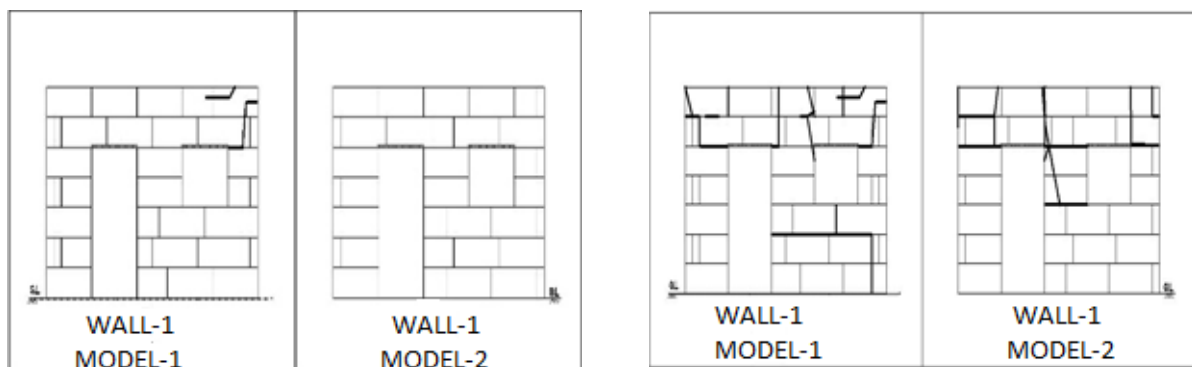
Table 5: Observations on Damage Patterns of Building Models under various shock loadings

Shock No. (Impact Angle)	Observations on Damage Patterns of Building Models
1 (15°)	<ul style="list-style-type: none"> • Most of the walls of models remain intact with no sign of damage. • Few minor vertical cracks observed at top layer of AAC blocks for wall-3 of building models due to load transferred through rigid diaphragm. • A vertical joint crack appeared at the top of the wall-2 of Model-1.
2 (15°)	<ul style="list-style-type: none"> • Wall-1, wall-2 and wall-3 of Model-1 suffered with few damages. • Wall-1 of Model-1 found with horizontal through cracks in AAC block due to horizontal shear and vertical mortar bed joint crack at right top corner.

	<ul style="list-style-type: none"> • Wall-2 of Model-1 showed vertical joint crack that propagates to cause through crack in AAC block due to out-of-plane bending of long wall-4. • Wall-3 of Model-1 subjected to vertical crack from top to bottom causing through crack in AAC block and vertical mortar bed joints crack. • Wall-3 and wall-4 of Model-2 resulted to very minor through cracks limited to the top course of AAC block walls.
3 (22.5°)	<ul style="list-style-type: none"> • Wall-3 of building models showed no progression in existing damage. • Wall-1 of Model-1 suffered with major mortar bed cracks at various locations above lintel and below sill level due to out-of-plane bending. • Wall-2 of Model-1 showed vertical joint and through crack at top left and right corner while wall-4 remained intact. • Wall-1 of Model-2 got vertical joint crack at top course of the AAC wall. • Wall-2 of Model-2 showed horizontal mortar bed joint crack between 2nd and 3rd course of the AAC wall.
4 (22.5°)	<ul style="list-style-type: none"> • Existing horizontal and vertical mortar bed crack progresses and new cracks appeared below sill level. • Wall-2 and wall-3 of Model-1 showed no progress in damage incurred. Wall-1 of Model-2 suffered with vertical and horizontal bed joint cracks above lintel level. • Wall-3 of Model-2 showed horizontal mortar bed joint cracks at 1st and 2nd course as well as between 2nd and 3rd course. • Wall-4 of Model-2 resulted to vertical joint cracks above and below window with vertical cracks at top left corner.
5 (30°)	<ul style="list-style-type: none"> • Wall-1 of Model-1 appeared with more horizontal and vertical mortar bed joint cracks below sill level of the window. • Wall-4 of Model-1 showed full horizontal mortar bed joint cracks at 3rd and 4th course with through cracks in the bottom left corner. • Wall-1 of Model-2 suffered with more horizontal mortar bed joint crack above lintel level. • Wall-4 and wall-2 of Model-2 progressed in horizontal and vertical mortar bed joint cracks above lintel level while no additional damage for wall-3.
6 (30°)	<ul style="list-style-type: none"> • Building models found to be in partial damaged state. • Wall-1 and wall-4 of building models showed more through cracks, horizontal and vertical mortar bed joints.
7 (37.5°)	<ul style="list-style-type: none"> • Wall-4 of Model-1 showed top to bottom vertical through crack between window to left walls junction and vertical mortar bed joint cracks. • Wall-1 of Model-1 got vertical and horizontal mortar bed joint cracks mostly above lintel level with few cracks below sill level as well. • Wall-3 of Model-1 showed vertical through crack up to bottom near right walls junction due to post-damage eccentricity of the lateral load. • Wall-4 of Model-2 progressed in vertical and horizontal mortar bed joint cracks mostly above lintel level. • Wall-1 of Model-2 subjected to more through cracks above lintel level, vertical and horizontal mortar bed joint cracks. • Dislodging of AAC block courses between door and window of the wall-1 of Model-2 started due to shearing action.
8 (37.5°)	<ul style="list-style-type: none"> • Horizontal and vertical mortar bed joint cracks appeared below sill level of the wall-4 of building models. • Wall-1 of Model-1 suffered with new through cracks limited to one to two courses, horizontal and vertical mortar bed joint cracks. • Widening of through and vertical mortar bed joint cracks for wall-4 of Model-1 observed. • Wall-4 of Model-2 subjected to more cracks above lintel level. • Dislodged AAC block courses of previous shock advanced to brink of fall.

9 (45°)	<ul style="list-style-type: none"> • Building models found to be in substantially damaged state. • Wall-1 of building models suffered with stepped type of failure below sill level. • Top two courses of building models showed dislodgement with sizeable lateral drift. • Wall-3 of Model-1 showed through cracks widened. • Horizontal and vertical cracks of wall-4 of Model-1 widened. • Building model-2 subjected to relatively more damage vis-à-vis Building Model-1. • Wall-2 of Model-2 sustained through cracks widen by ~ 30 mm leading to junction separation with wall-1. • Wall-3 of Model-2 observed with two AAC block courses dislodged due to higher out-of-plane vibration modes. • Horizontal and vertical mortar bed joint cracks opened-up throughout length for wall-4 of Model-2 with top AAC block courses get dislodged. • Extensive damage to the building models leading to loss of structural integrity but have not collapsed.
10 (45°)	<ul style="list-style-type: none"> • Wall-3 of Model-1 collapsed completely with only bottom two AAC block courses remained intact. • Wall-1 of Model-1 showed part failure from top corner of the window to the top of right wall junction. • Wall-1 of Model-1 showed stepped failure below sill level with bending visibly evident. • Wall-2 of Model-1 suffered with through cracks near the junctions with wall-1 and wall-4 that widened with visible wall bending. • Wall-1 and wall-4 of Model-2 showed through cracks that widened and top AAC blocks courses tried to get dislodged. • Lintel above the window of the Model-2 found to be broken with walls visibly bent in second mode of vibration. • Top AAC block course of wall-3 and wall-2 of Model-2 completely dislodged. • Building Model-2 survived with heavy damages.

Figure 7(a) to Figure 7(d) shows crack pattern observed for walls; wall-1 to wall-4 of the building models constructed with AAC blocks to the representative shocks applied through pendulum released from 15° to 45° degrees as discussed above.



(a)

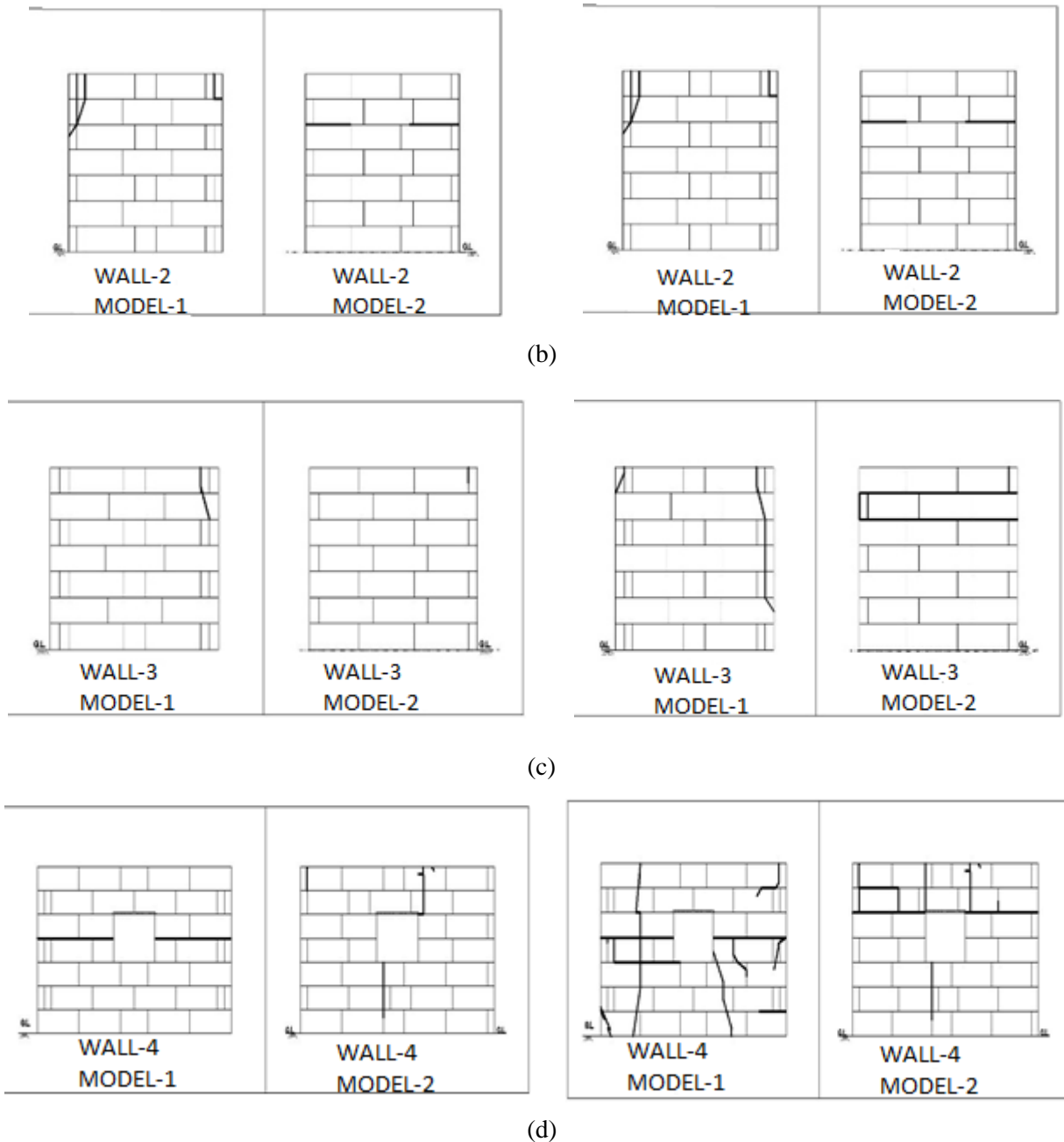


Fig. 7 Damage in the Representative Walls (a) Wall-1, (b) Wall-2, (c) Wall-3, and (d) Wall-4 of Building Models subjected to Shock with various Incident Angles

It is evident from Figure 7(a) to Figure 7(d) that both building models were suffered with through cracks in the AAC blocks as well as cracks in horizontal and vertical mortar bed joints across the height of the models. It has been observed that AAC building Model-2 built with stretcher bond withstand dynamic shocks relatively better than AAC building Model-1 built with English bond which suffered severe damages in various walls before it was collapsed.

Figure 8(a) to Figure 8(d) shows representative real time photographs captured at various stages of dynamic testing on building models built through AAC blocks.



(a)



(b)



(c)



(d)

Fig. 8 Real Time Photographs of AAC Building Models with Damages in the Walls (a), Wall-1 (b), Wall-2 (c), Wall-3, and (d) Wall-4

CONCLUSIONS

Masonry buildings are a common typology adopted in rural and semi-urban areas world-wide due to their good resistance against gravity loads and cost affordability. However, such building were found to be weak against seismic loading and suffered to severe damage during past earthquakes. Otherwise mostly used red-clay bricks are getting rapidly replaced by Autoclaved Aerated Concrete (AAC) blocks in the construction industry due to its distinct advantages of light weight and speed of construction. AAC blocks are widely employed as non-structural masonry infill in Reinforced Concrete (RC) frame, hitherto its use in semi-engineered masonry building construction has not been explored. Two building models; one with English and other with stretcher bond are constructed using AAC blocks on unique Shock Table facility. Rigid diaphragm action is ensured through specially fabricated modular slab assembly. Uniaxial accelerometers are attached at top of the walls in perpendicular direction to incident shock and on concrete table to measure acceleration response and input acceleration, respectively. Each building model are critically observed after each shock for damaged suffered to understand its dynamic behavior.

It has been observed that AAC block based building models reduce construction time to half as compared to red-clay brick based building models of similar order. Building model-2 built with stretcher bond is found to survive all (10 nos.) shocks with heavy damage while wall-3 of Model-1 built with English bond completely collapsed alongside partial collapse of wall-1. It is observed through present study that building model built with stretcher bond shows relatively better dynamic performance vis-à-vis English bond based building model. During dynamic testing, building models were observed with through cracks in the AAC block based courses of various walls indicating existence of good bond between AAC blocks and binding material. Out-of-plane bending failure observed in the walls; wall-1 and wall-4 of building models establishes that it is a predominant mode of failure is such types of masonry buildings. Non-uniform degradation in wall rigidities resisting lateral load due to shock loading might lead further damage to building models due to eccentricities produced as seen from the failure of wall-3 for building model-1. It has been found that building models built with AAC unit blocks have performed at par with red-clay based building models on the basis of qualitative parameters of extent and pattern of damage suffered when compared with experimental results obtained for similar types of building models tested in the past. However, life hazard reduces relatively with AAC block masonry building due to light weight AAC block. Retrofitting strategies for seismic performance enhancement of AAC block masonry building models may be evolved on similar lines that of red-clay brick masonry building.

ACKNOWLEDGEMENTS

Authors would like to acknowledge the support of Brixo Industries, Ahmedabad for providing commercial Autoclaved Aerated Concrete (AAC) block used in the construction of building models. Technical support received from Mr. Pawan Pandey, Junior Research Fellow at Civil Engineering Department, School of Engineering, Institute of Technology, Nirma University, Ahmedabad for analysis of experimental data is deeply appreciated.

REFERENCES

1. IS:2185-3 (1984). "Specification for Concrete Masonry Units", *Bureau of Indian Standards, New Delhi*.
2. Bose, S. and Rai, D.C. (2014). "Behavior of AAC Infilled RC Frame under Lateral Loading", *Tenth U. S. National Conference on Earthquake Engineering, Frontiers of Earthquake Engineering, Alaska, July 21-25*.
3. Sucuoğlu, H. and Siddiqui, U.A. (2014). "Pseudo-dynamic Testing and Analytical Modelling of AAC Infilled RC Frames", *Journal of Earthquake Engineering, Vol. 18, No. 8, pp. 1281-1301*.
4. Schwarz, S., Hanaor, A. and Yankelevsky, D.Z. (2015). "Experimental Response of Reinforced Concrete Frames with AAC Masonry Infill Walls to In-plane Cyclic Loading", *Structures, Vol. 3, pp. 306-319*.

5. Mehrabi, A.B., Benson, S.P., Schuller, M.P. and Noland, J.L. (1996). "Experimental Evaluation of Masonry-Infilled RC Frames", *Journal of Structural Engineering*, Vol. 122, No. 3, pp. 228-237.
6. Bhoraniya, T.H. and Purohit, S.P. (2020). "Post-yield Damping Ratio Estimation Studies for Masonry-Infilled Reinforced Concrete Frames", *Iranian Journal of Science and Technology, Transaction of Civil Engineering*, Vol. 44, Vol. Suppl. 1, pp. S193-S204.
7. Jiang, H., Liu, X. and Mao, J. (2015). "Full-scale Experimental Study on Masonry Infilled RC Moment-Resisting Frames under Cyclic Loads", *Engineering Structures*, Vol. 91, pp. 70-84.
8. Ersubas, F. and Korkmaz, H. (2010). "Shaking Table Tests on Strengthening of Masonry Structures against Earthquake Hazard", *Natural Hazards and Earth System Sciences*, Vol. 10, pp. 1209-1220.
9. Ghezelbash, A., Beyer., K., Dolatshahi., K.M. and Yekrangnia M. (2020). "Shake Table Test of a Masonry Building Retrofitted with Shotcrete", *Engineering Structures*, Vol. 219, pp. 110912.
10. Costa, A.A., Penna, A. and Magenes, G. (2011). "Seismic Performance of Autoclaved Aerated Concrete (AAC) Masonry: From Experimental Testing of the In-plane Capacity of Walls to Building Response Simulation", *Journal of Earthquake Engineering*, Vol. 15, No. 1, pp.1-31.
11. Elmalich, D. and Rabinovitch, O. (2012). "In-Plane Dynamic Excitation of AAC Masonry Walls Patched with FRP: Dynamic Testing and Analysis", *Journal of Mechanics of Materials and Structures*, Vol. 7, No. 7, pp. 657-686.
12. Miccoli, L. (2018). "Seismic Performances of AAC Masonry: A Review of Experimental and Numerical Approaches", *ce/papers*, Vol. 2, No. 4, pp. 301-309.
13. Gokmen, F., Binici, B., Canbay, E., Alemir, A., Ogdu M.K., Uzgan, U., Eryurtlu, Z. and Ozdemir, G. (2018). "In Situ Seismic Testing of a Reinforced Autoclaved Aerated Concrete Building", *Mauerwerk, European Journal of Masonry*, Vol. 22, No. 5, pp. 305-313.
14. Marino, S., Cattari, S., Lagomarsino, S., Dizhur D. and Ingham, J.M. (2019). "Post-earthquake Damage Simulation of Two Colonial Unreinforced Clay Brick Masonry Buildings Using Equivalent Frame Method", *Structures*, Vol. 19, pp. 212-226.
15. Nayak, S. and Dutta, S.C. (2016). "Failure of Masonry Structures in Earthquake: A Few Simple Cost Effective Techniques as Possible Solution", *Engineering Structures*, Vol. 106, pp. 53-67.
16. Chourasia, A., Bhattacharyya, S.K., Bhandari, N.M. and Bhargava, P. (2016). "Seismic Performance of Different Masonry Buildings: Full-Scale Experimental Study", *Journal of Performance of Constructed Facilities, ASCE*, Vol. 30, No. 5, pp. 1-10.
17. Kadam. S.B. and Singh. Y. (2020). "Experimental Investigations on Masonry Buildings Strengthened Using Ferro-Cement Overlay Under Dynamic Loading", *ISET Journal of Earthquake Technology, Paper No. 548, Vol. 57, No. 1, pp. 1-16.*
18. Pathak. J., Patwari, N.N. and Sarma. B. (2020). "A Comparative Prognostic Damage Scenario of Non-Engineered Masonry and Traditional Assam Type Housing in Guwahati Urban Centre", *ISET Journal of Earthquake Technology, Paper No. 551, Vol. 57, No. 1, pp. 43-59.*
19. IS:6441-IV (1972). "Methods of Test for Autoclaved Cellular Concrete Products", *Bureau of Indian Standards, New Delhi.*
20. Jagadish, K.S. (2015). "Structural Masonry", *I.K. International Publishing House Pvt. Ltd., New Delhi, India.*
21. Sharma, S., Soni, D. and Purohit, S.P. (2018). "Mechanical Properties of Red Clay Bricks under Compression and Shear: An Experimental and Numerical Investigation", *XIth Structural Engineering Convention (SEC18), Department of Civil Engineering, Jadavpur University, Kolkata, pp. 187-193.*
22. IS:2250 (1993). "Code of Practice for Preparation and Use of Masonry Mortars", *Bureau of Indian Standards, New Delhi.*
23. National Center for Peoples' Action in Disaster Preparedness (2005). "Demonstration of Earthquake Resistance Design for Stone and Brick Masonry Building through Shock Table Testing", *Project Report Department of Science and Technology, New Delhi.*